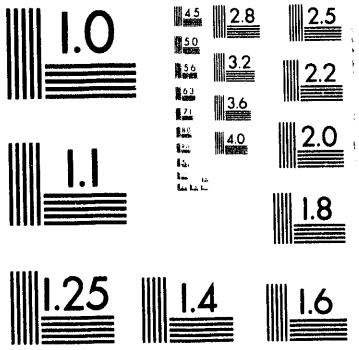
1.0
2.8
2.5
3.2
2.2
3.6
4.0
2.0
1.1
1.8
1.25
1.4
1.6

1 of 1

DOE/PC/88801--T10

IMPROVED PERFORMANCE IN COPROCESSING THROUGH FUNDAMENTAL AND MECHANISTIC STUDIES IN HYDROGEN TRANSFER AND CATALYSIS

Contract No. DE-AC22-88PC88801

Quarterly Report

March 27, 1991 - June 26, 1991

Christine W. Curtis

Department of Chemical Engineering
Auburn University, AL 36849-5127

MASTER

DISCLAIMER

This report was prepared as an account of work sponsored by an agency of the United States Government. Neither the United States Government nor any agency thereof, nor any of their employees, makes any warranty, express or implied, or assumes any legal liability or responsibility for the accuracy, completeness, or usefulness of any information, apparatus, product, or process disclosed, or represents that its use would not infringe privately owned rights. Reference herein to any specific commercial product, process, or service by trade name, trademark, manufacturer, or otherwise does not necessarily constitute or imply its endorsement, recommendation, or favoring by the United States Government or any agency thereof. The views and opinions of authors expressed herein do not necessarily state or reflect those of the United States Government or any agency thereof.

DISTRIBUTION OF THIS DOCUMENT IS UNLIMITED

IMPROVED PERFORMANCE IN COPROCESSING THROUGH FUNDAMENTAL AND MECHANISTIC STUDIES IN HYDROGEN TRANSFER AND CATALYSIS

Quarterly Report

March 27, 1991 - June 26, 1991

Submitted by

DEPARTMENT OF CHEMICAL ENGINEERING
AUBURN UNIVERSITY, ALABAMA

Dr. Christine W. Curtis, Principal Investigator

Nb42/2Q91COPRO.RPT

ACKNOWLEDGEMENTS

The experimental work of Ruth Owens, Honggon Kim, Michael Bedell, S. L. Wang and Dr. Kenneth Olson is sincerely appreciated. The technical assistance of Franklin Bowers and Joseph Aderholdt is gratefully acknowledged.

TABLE OF CONTENTS

Objective 1

Major Subtasks and Their Objectives 1

Introduction 1

Experimental Work 2

Task I. Elucidation of Hydrogen Transfer Reactions in Coprocessing 2

Subtask I.A. Hydrogen Transfer from Cycloalkanes 2

Subtask I.B. Pretreatment of Petroleum Residua for Enhanced Hydrogen Transfer 2

Subtask I.B.1. Pretreatment, Fractionation and Reactivity of Petroleum Residua 2

Task II. Development of Potent Nonaromatic Hydroaromatic Donors for Coprocessing 3

Subtask II.C. Production of Nonaromatic Hydroaromatics in Real Solvent Systems 3

Introduction 3

Experimental 3

Results and Discussion 4

Subtask II.D. Chemistry and Reactivity of Nonaromatic Hydroaromatic Enriched Petroleum Solvents 11

Thermal Reaction Product Slates 11

Kinetics Analysis and Arrhenius Plots for Thermal Reaction of the Compounds under Nitrogen and Hydrogen 15

Determination of Gibbs Free Energy for the Thermal Reactions 16

LIST OF TABLES

II.C.1. Comparison of Percent Coal Conversion to THF Solubles using Birch-pretreated Residua, Original Residua, and Original Residua Plus Isotetralin 6

II.D.1. Thermal Reaction Products from Isotetralin at 225°C 19

II.D.2 Thermal Reaction Products from Isotetralin at 300°C 19

II.D.3. Thermal Reaction Products from Isotetralin at 380°C 20

II.D.4. Thermal Reaction Products from Tetralin at 380°C 20

II.D.5. Thermal Reaction Products from Tetralin at 425°C 21

II.D.6. Thermal Reaction Products from Tetralin at 450°C 21

II.D.7. Thermal Reaction Products from Octahydroanthracene at 425°C 22

II.D.8. Thermal Reaction Products from Octahydroanthracene at 450°C 22

II.D.9. Thermal Reaction Products from Octahydroanthracene at 475°C 23

II.D.10. Thermal Reaction Products from Dihydroanthracene at 380°C 23

II.D.11. Thermal Reaction Products from Dihydroanthracene at 425°C 24

II.D.12. Thermal Reaction Products from Dihydroanthracene at 450°C 24

II.D.13. Thermal Reaction Products from Hexahydroanthracene at 225°C 25

II.D.14. Thermal Reaction Products from Hexahydroanthracene at 300°C 25

II.D.15. Thermal Reaction Products from Hexahydroanthracene at 380°C 26

II.D.16. Apparent Rate Constants and Arrhenius Parameters for the Model Compound Reactivity Studies 27

LIST OF FIGURES

Figure II.C.1. Comparative UV-VIS Spectra for Maya Residuum 7

Figure II.C.2. Comparative UV-VIS Spectra for DAU Rock Residuum 8

Figure II.C.3. Comparative UV-VIS Spectra for South Louisiana Residuum 9

Figure II.C.4. Comparative FTIR Spectra for DAU Rock Residuum 10

Figure II.D.1. Plot of Gibbs Free Energy vs Temperature Nitrogen Atmosphere 28

Figure II.D.2. Plot of Gibbs Free Energy vs. Temperature Hydrogen Atmosphere 29

IMPROVED PERFORMANCE IN COPROCESSING THROUGH FUNDAMENTAL AND MECHANISTIC STUDIES IN HYDROGEN TRANSFER AND CATALYSIS

OBJECTIVE

To gain a fundamental understanding of the role and importance of hydrogen transfer reactions in thermal and catalytic coprocessing by examining possible hydrogen donation from cycloalkane/aromatic systems and by understanding the chemistry and enhanced reactivity of hydrotreated residuum, as well as by enriching petroleum solvent with potent new donors, nonaromatic hydroaromatics, thereby promoting hydrogen transfer reactions in coprocessing.

MAJOR TASKS AND THEIR OBJECTIVES

Task I. Elucidation of Hydrogen Transfer Reactions in Coprocessing

Objective. To attain fundamental understanding of the hydrogen transfer reactions which occur during coprocessing and to elucidate their role and importance in achieving upgraded products.

Task II. Development of Potent Nonaromatic Hydroaromatic Hydrogen Donors for Coprocessing

Objective. To generate petroleum solvents enriched with nonaromatic hydroaromatics by metal or electrochemical reduction and to evaluate their reactivity and selectivity.

INTRODUCTION

Research continued this quarter on Subtask I.A., Hydrogen Transfer from Cycloalkanes, Subtask I.B.1., Pretreatment, Fractionation, and Reactivity of Petroleum Residua, Subtask II.A., Synthesis of Nonaromatic Hydroaromatics by Reduction with Metals and Electroreduction, and Subtask II.,D., Chemistry and Reactivity of Nonaromatic Hydroaromatic Enriched Petroleum Solvents.

EXPERIMENTAL WORK

TASK I. ELUCIDATION OF HYDROGEN TRANSFER REACTIONS IN COPROCESSING

SUBTASK I.A. HYDROGEN TRANSFER FROM CYCLOALKANES

During this quarter, all research on this subtask was completed, and the data obtained from coprocessing and model compound reactions designed to investigate hydrogen transfer from cycloalkanes to aromatics were tabulated and analyzed. All results obtained from the analysis of data from the various combinations of model compound/petroleum residuum/coal reactions performed for this subtask will be reported in detail in the final report.

In addition, during the quarter, a preprint which involves the research performed under this subtask was submitted to the Fuel Chemistry Division of the American Chemical Society for future presentation at the Third International Chemical Congress in New York. Also this quarter, Dr. Curtis attended the Joint DOE/CANMET Meeting in Atlanta and present results from the research performed under this subtask.

SUBTASK I.B. PRETREATMENT OF PETROLEUM RESIDUA FOR ENHANCED HYDROGEN TRANSFER

SUBTASK I.B.1. PRETREATMENT, FRACTIONATION AND REACTIVITY OF PETROLEUM RESIDUA

During this quarter, all research on this subtask was completed, and the data obtained from thermal coprocessing reactions of coal with untreated residuum, thermally pretreated residuum, catalytically pretreated residuum, fractionated untreated residuum, fractionated thermally pretreated residuum, and fractionated catalytically pretreated residuum were tabulated

and analyzed. All results determined from the analysis of the data obtained from the research performed under this subtask will be reported in detail in the final report.

In addition, during this quarter, selected data obtained from the research performed under this subtask was used in the preparation of manuscripts which will be submitted for publication in the near future.

TASK II. DEVELOPMENT OF POTENT NONAROMATIC HYDROAROMATIC DONORS FOR COPROCESSING

SUBTASK II.C. PRODUCTION OF NONAROMATIC HYDROAROMATICS IN REAL SOLVENT SYSTEMS

INTRODUCTION

The objective of this subtask is to produce nonaromatic hydroaromatic compounds in atmospheric or vacuum residua by electroreduction or reduction with metals. The Birch reduction method was chosen because the method had been very successful in reducing naphthalene with sodium metal to produce high purity 1,4,5,8-tetrahydronaphthalene (isotetralin). A modified Birch reduction designed to produce nonaromatic hydroaromatic compounds in petroleum residua was performed initially. Research using electroreduction for the synthesis of nonaromatic hydroaromatic compounds by electroreduction will not proceed in this contract because the Birch method was highly successful in producing the reduced resids needed in this research.

EXPERIMENTAL

This quarter, the experimental conditions for the Birch reduction of the aromatic compound, naphthalene, to produce the nonaromatic compound, isotetralin, were modified in

the Birch reduction of DAU Rock residuum and South Louisiana residuum. Tetrahydrofuan (THF), a cyclic ether, was substituted for ethyl ether as a solvent for DAU Rock residuum and South Louisiana residuum because of the low solubility of these residua in ethyl ether.

Subsequent to Birch reduction of both the DAU Rock and the South Louisiana residua and the addition of three liters of distilled water to the reaction mixture, it was possible to separate the organic (THF) phase from the aqueous phase. Distilled water was added to the separated organic phase and the mixture was distilled to a temperature (79°C) just sufficient to remove the methanol, THF, and ethanol (B.P. 78°C) from the Birch-reduced DAU Rock and South Louisiana residua. The distilled water was then separated from each residuum, and each residuum was washed four times with distilled water and dried at reduced pressure under a nitrogen atmosphere prior to reaction with coals or spectral analysis.

RESULTS AND DISCUSSION

Most significantly during this quarter, Birch-pretreated DAU Rock residuum and Birch-pretreated South Louisiana residuum was reacted with Pittsburgh No. 8 coal with excellent results. The percent coal conversion to THF solubles for Pittsburgh No. 8 coal reacted with Birch-pretreated DAU Rock and South Louisiana residua, original (untreated) DAU Rock and South Louisiana residua, and original DAU Rock and South Louisiana residua plus isotetralin are presented in Table II.C.1. The previously reported data for Birch-pretreated Maya residuum, original Maya residuum, and original Maya residuum plus isotetralin reacted with Pittsburgh No. 8, Western Kentucky No. 9 and Upper Freeport coals are also presented in Table II.C.1 for comparison.

The data indicated that Birch-pretreated DAU Rock residuum and Birch-pretreated South Louisiana residuum performed in a highly efficient manner compared to original (untreated) DAU Rock residuum and original South Louisiana residuum, and in a comparable manner to original DAU Rock residuum plus isotetralin, and original South Louisiana residuum plus isotetralin when reacted with a reactive coal such as Pittsburgh No. 8 coal. Increases in percent coal conversion of approximately seven and six percent were observed for Birch-pretreated DAU Rock residuum and Birch-pretreated South Louisiana residuum, respectively, when compared to original DAU rock residuum and original South Louisiana residuum.

Also this quarter, ultraviolet-visible (UV-VIS) spectra for Birch-reduced petroleum residua (Maya, DAU Rock and South Louisiana) were each compared with UV-VIS spectra for their original (untreated) petroleum residua (Maya, DAU Rock, and South Louisiana). The comparative spectra obtained from THF dissolution of equal weights of Birch-pretreated and original residua are presented in Figures II.C.1 through II.C.3. For each set of spectra, the Birch-pretreated residuum absorbance clearly exceeds the original residuum absorbance.

Fourier transform infrared (FTIR) comparative spectra obtained this quarter from carbon tetrachloride dissolution of equal weights of Birch-pretreated DAU Rock and original DAU Rock residua are shown in Figure II.C.4. The spectra indicate that Birch-reduction of DAU Rock residuum resulted in an increase in methyl carbons in the residuum compared to methylene carbons. This change was expected since chemical reduction should result in a net gain of hydrogen in the molecules undergoing reduction.

Table II.C.1. Comparison of Percent Coal Conversion to THF Solubles using Birch-pretreated Residua, Original Residua, and Original Residua Plus Isotetralin

Coal	Percent Coal Conversion		
	Pretreated Maya	Original Maya	Original Maya Plus Isotetralin
Pittsburgh No. 8	43.3(2.6)[1]	20.1(3.3)	41.5(0.6)
W. Kentucky No. 9	43.7(2.9)	24.3(3.3)	44.8(0.3)
Upper Freeport	16.9(0.8	14.0(1.6)	16.5(3.4)
	Pretreated DAU Rock	Original DAU Rock	Original DAU Rock Plus Isotetralin
Pittsburgh No. 8	47.0(1.8)	39.6(1.9)	45.6(0.5)
	Pretreated S. LA[2]	Original S. LA	Original S. LA Plus Isotetralin
Pittsburgh No. 8	31.4(1.7)	25.1(3.2)	33.8(3.7)

[1] Percent coal conversion followed by percent standard deviation in parentheses
[2] S. LA is South Louisiana resid.

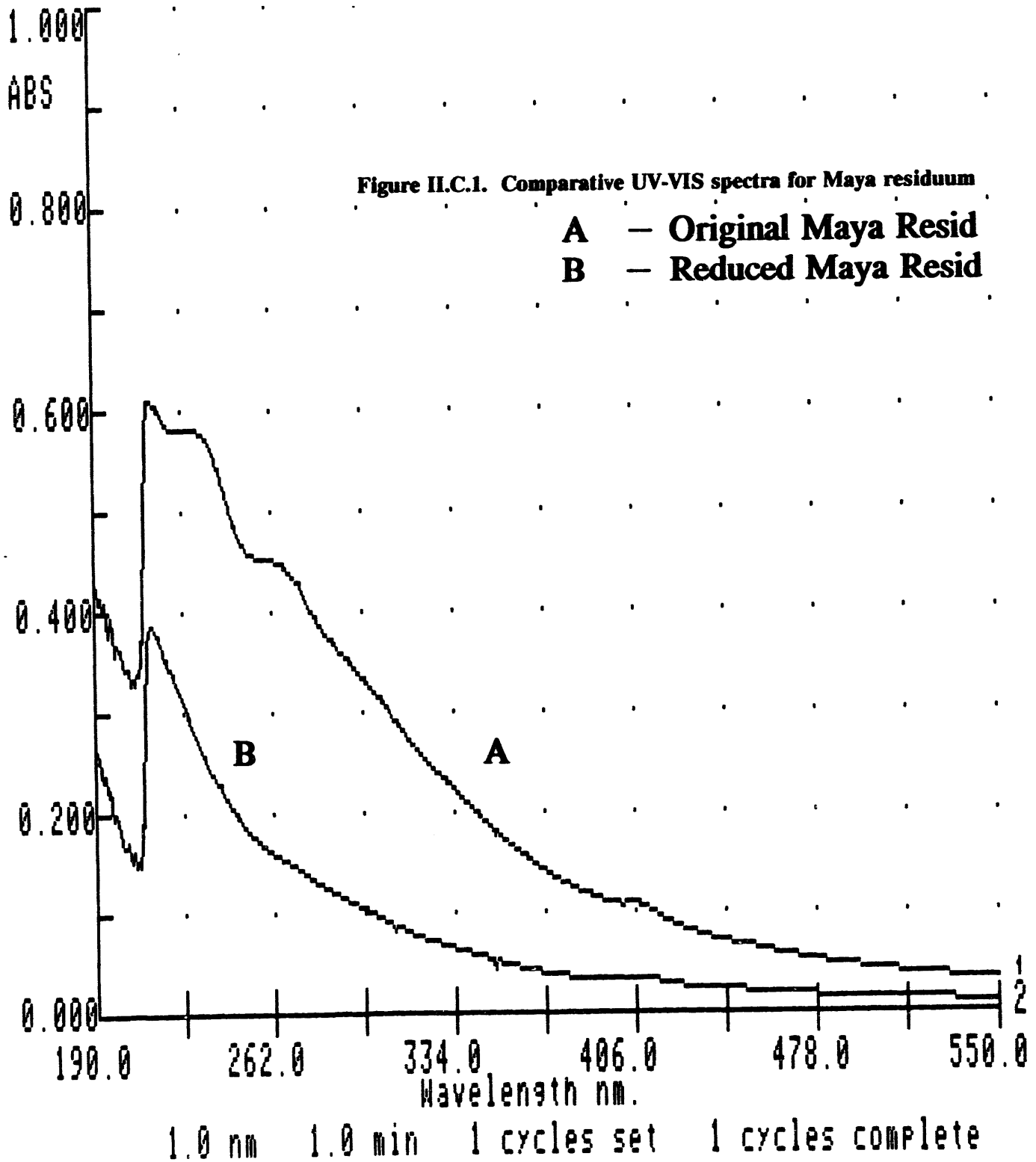

Figure II.C.1. Comparative UV-VIS spectra for Maya residuum

A — Original Maya Resid
B — Reduced Maya Resid

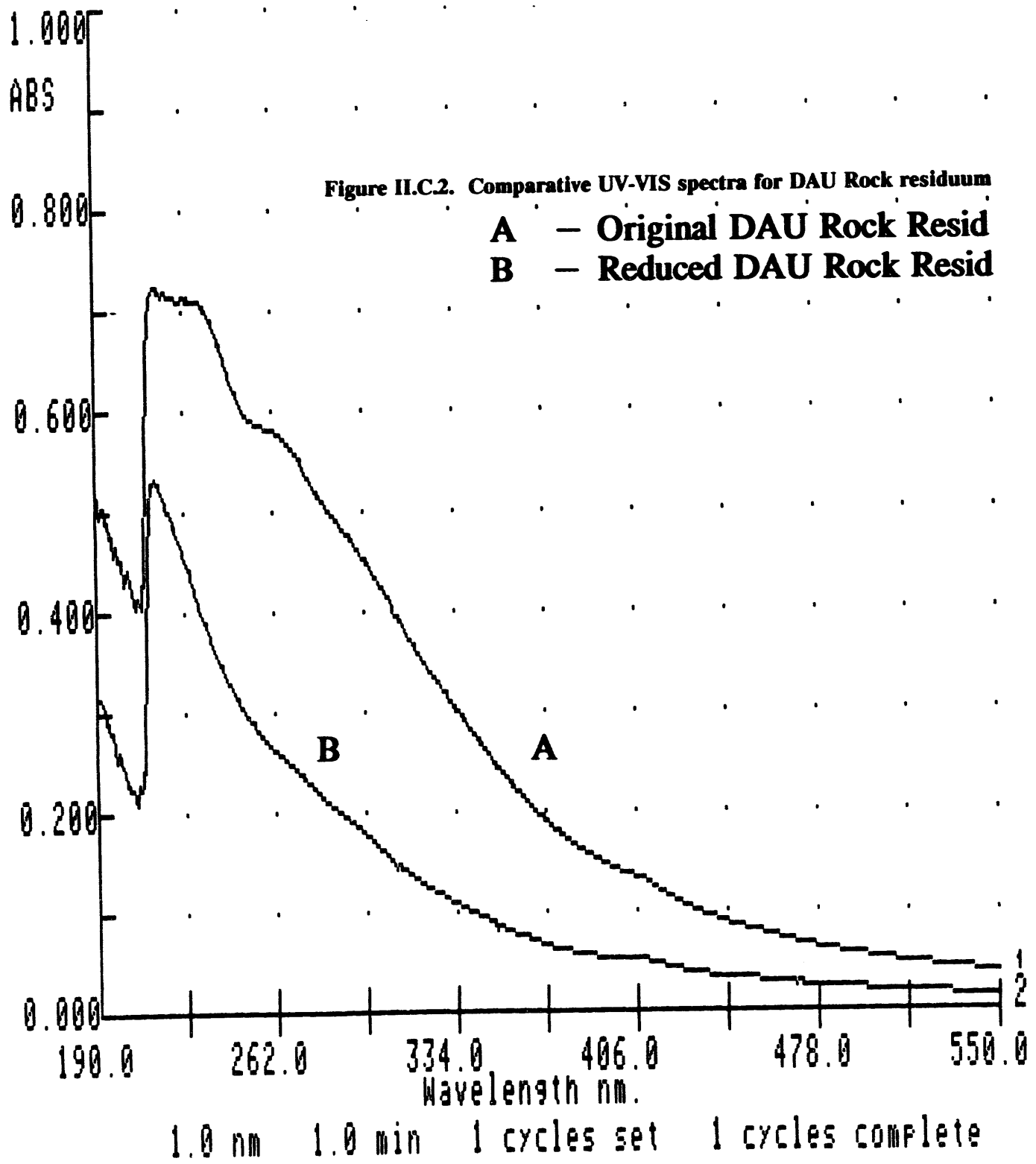

Figure II.C.2. Comparative UV-VIS spectra for DAU Rock residuum

A – Original DAU Rock Resid
B – Reduced DAU Rock Resid

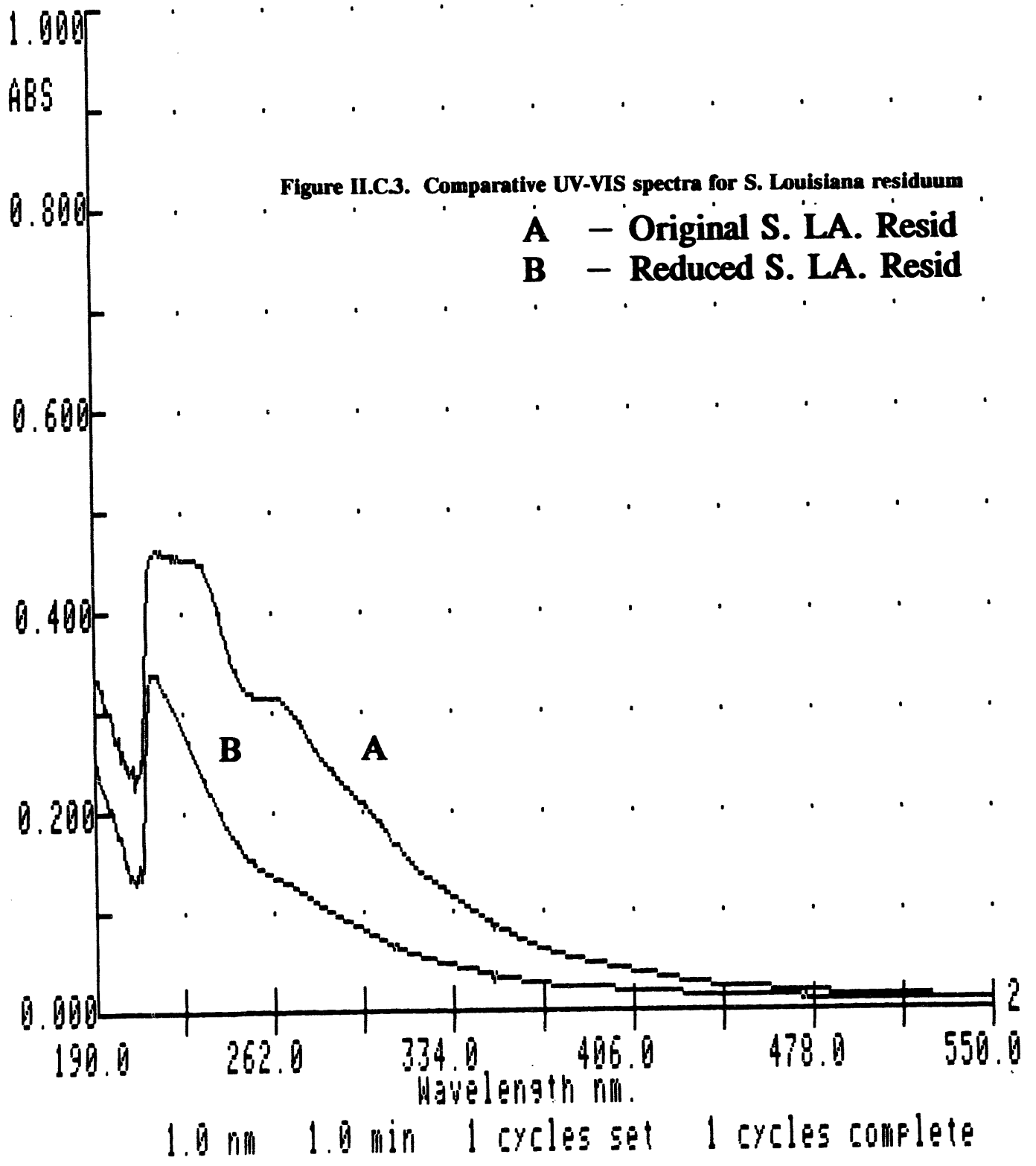

Figure II.C.3. Comparative UV-VIS spectra for S. Louisiana residuum

A – Original S. LA. Resid
B – Reduced S. LA. Resid

Figure II.C.4. Comparative FTIR spectra for DAU Rock residuum

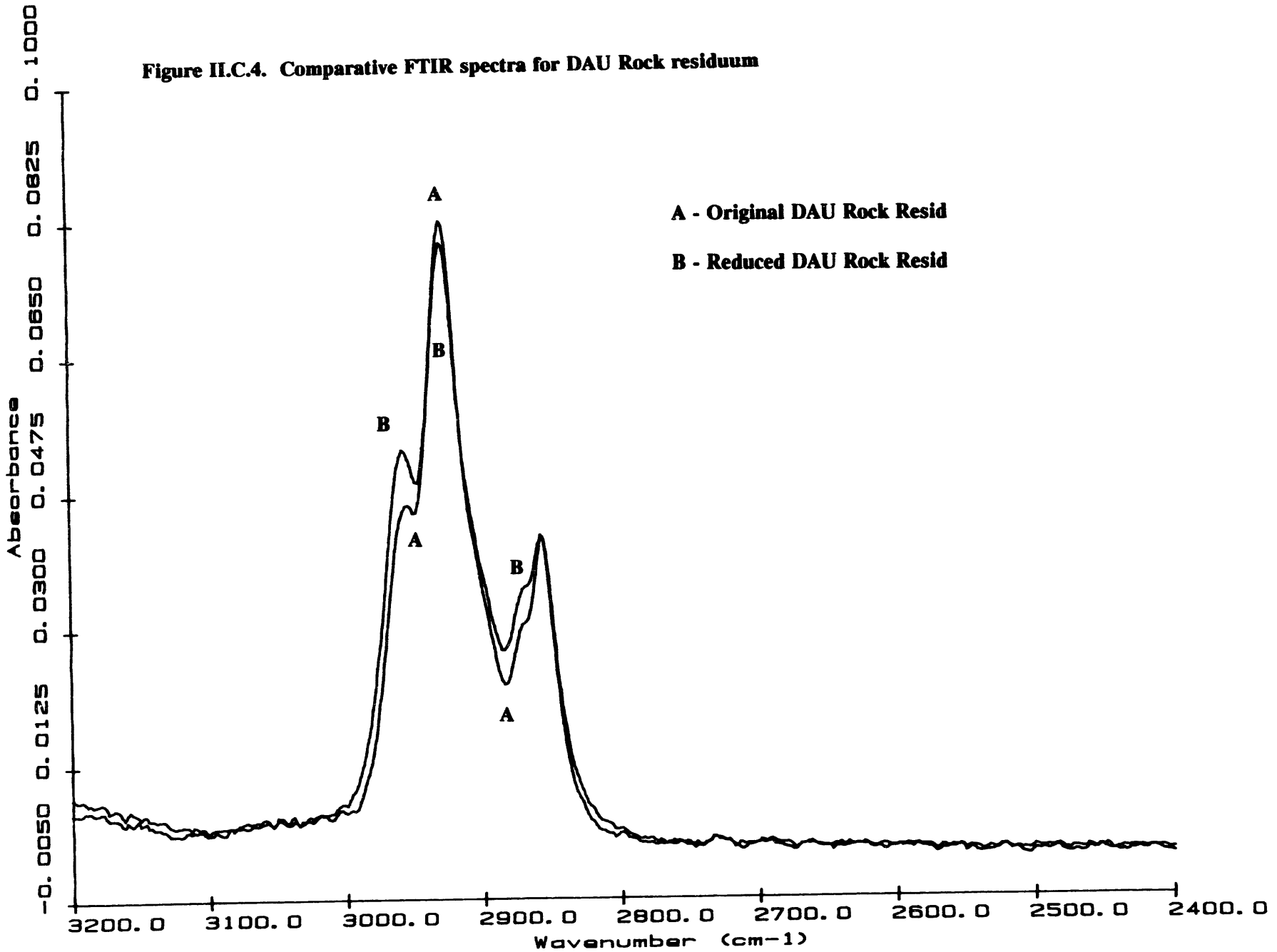

SUBTASK II.D. CHEMISTRY AND REACTIVITY OF NONAROMATIC HYDROAROMATIC ENRICHED PETROLEUM SOLVENTS

THERMAL REACTION PRODUCT SLATES

The first stage of research this quarter for the kinetic analysis of the nonaromatic hydroaromatics and their conventional hydrogen donor compounds consisted of thermally reacting the individual compounds at various reaction times at three different temperatures. There were up to seven reaction times, including $\lambda=0$ at $t=0$, used in the fit to first-order reaction kinetics under both nitrogen and hydrogen atmospheres with a given compound at a single temperature. Tables II.D.1 through II.D.15 present the results that were obtained in the model compound reactivity studies for isotetralin (ISO), tetralin (TET), hexahydroanthracene (HHA), octahydroanthracene (OHA), and dihydroanthracene (DHA).

1,4-Dihydronaphthalene (DHN) was the only reaction product formed from ISO in the reactions under both nitrogen and hydrogen at 225°C (Table II.D.1). With a reaction time of 90 minutes, ISO remained 95.7% unconverted under hydrogen and with a reaction time of 120 minutes remained 92.2% unreacted under nitrogen. In a hydrogen atmosphere at 300°C (Table II.D.2), 1,4-DHN was the primary reaction product from ISO, with a minor amount of 1,2-DHN and TET being formed with longer reaction times. In a nitrogen atmosphere, 1,4-DHN was the only product, except in the 2 minute reaction time where NAP and 1,2-DHN were also formed, in an amount of less than 1% each. With a reaction time of 90 minutes, ISO remained 52.7% unreacted under hydrogen and 69.1% unconverted under nitrogen. For the reactions of ISO in a hydrogen atmosphere at 380°C (Table II.D.3) a more varied product slate was obtained. ISO was completely converted within the first 15 minutes. At the short reaction times, 1,4-DHN and naphthalene (NAP) were the predominant reaction products, with lesser amounts of TET and

1,2-DHN formed. At reaction times greater than 15 minutes, NAP became the predominant reaction product. In a nitrogen atmosphere, ISO was more than 98% converted within the first 15 minutes of the reaction, primarily to 1,4-DHN and NAP, with less than 5% TET and 1,2-DHN formed. As the reaction times increased, the amount of NAP formed increased to ~72 % at a reaction time of 60 minutes.

In the reactions with TET at 380°C (Table II.D.4) in a hydrogen atmosphere the products consisted of NAP, 1,2-DHN, 1,4-DHN, and trans-decalin (t-DEC). In a nitrogen atmosphere the same products were observed, except no t-DEC was produced. With a reaction time of 90 minutes, TET was less than 15% reacted under hydrogen and less than 7% reacted under nitrogen. In the reactions of TET at 425°C, the results of which are shown in Table II.D.5, 1,2-DHN and 1,4-DHN were the predominant products, with a minor amount of NAP being formed. As the reaction times increased, the amount of 1,4-DHN recovered also increased. However, the results of previous work by Bedell and Curtis (1991) suggested that TET first dehydrogenated to 1,2-DHN which then isomerized to form 1,4-DHN. At a reaction time of 60 minutes, TET reacted substantially leaving 30.3% unreacted under hydrogen and 32.6% unreacted under hydrogen. 1,4-DHN and 1,2-DHN were the predominant reaction products from TET at 450°C (Table II.D.6) under hydrogen. As the reaction times increased to 90 minutes, 1,4-DHN became the predominant product and TET converted by more than 90%. In a nitrogen atmosphere, 1,4-DHN and 1,2-DHN dominated the reaction products at the shorter reaction times; however, at a reaction time of 60 minutes, NAP was the primary reaction product. TET was 89.6% reacted at a reaction time of 60 minutes under nitrogen.

Tables II.D.7 through II.D.15 present the results of the thermal reaction of the three-ring hydrogen donor compounds, e.g. OHA, DHA, and HHA. As can be seen in Table II.D.7, OHA was substantially unreactive, being less than 15% converted under both nitrogen and hydrogen at reaction times up to 60 minutes. The reaction products formed were DHA, tetrahydroanthracene (THA), and anthracene (ANT). At a reaction temperature of 450°C, as shown in Table II.D.8, the predominant reaction product was THA, with lesser amounts of DHA and ANT being formed. OHA remained 43.4% unconverted under hydrogen and 59.2% unreacted under nitrogen with a reaction time of 60 minutes. With a reaction temperature of 475°C (Table II.D.9), OHA was more than 85% converted under both nitrogen and hydrogen with a reaction time of 60 minutes. At this higher temperature, DHA and THA were the primary reaction products, with a lesser amount of ANT being formed.

Table II.D.10 presents the results for the reactions of DHA at 380°C. DHA was less than 15% converted under hydrogen to approximately equal amounts of THA and ANT with a reaction time of 90 minutes. In a nitrogen atmosphere and 60 minute reaction time DHA was converted less than 10%, with ANT being the only reaction product. At a reaction temperature of 425°C (Table II.D.11), DHA was less than 15% converted in a hydrogen atmosphere at a reaction time of 90 minutes, while being more than 60% converted in 60 minutes under nitrogen. Under both nitrogen and hydrogen, ANT was the only reaction product formed, except at 60 minutes under hydrogen where 3.2% THA was recovered. DHA was 71.3% unconverted at 450°C under hydrogen, while being only 6.6% unconverted under nitrogen at the longest reaction time used of 60 minutes (Table II.D.12). The primary reaction product was

ANT, with a lesser amount of THA being produced in a hydrogen atmosphere and ~2% THA being formed at 60 minutes under nitrogen.

At 225°C (Table II.D.13) HHA was less than 10% converted to THA and DHA at reaction times up to 120 minutes under hydrogen, and less than 15% converted under nitrogen in reaction times up to 90 minutes. In the reactions under both nitrogen and hydrogen and reaction times up to 60 minutes, HHA at 300°C (Table II.D.14) produced DHA as the primary reaction product, with a lesser amount of THA being formed. HHA was 60.4% unconverted under hydrogen and 58.7% unconverted under nitrogen with a reaction time of 60 minutes. At a temperature of 380°C (Table II.D.15) HHA was 90% converted under hydrogen with a reaction time of 15 minutes and was more than 98% converted at a reaction time of 60 minutes. In a nitrogen atmosphere, HHA was 98% converted in 15 minutes. The primary reaction product under both nitrogen and hydrogen was DHA, with a lesser amount of THA and ANT being formed.

As can be seen by examining the reaction data presented in Tables II.D.1 through II.D.15, the two nonaromatic hydroaromatics, ISO and HHA, were much more reactive than their conventional hydrogen donor analogues, TET, OHA, and DHA. The nonaromatic hydroaromatics reacted at much lower temperatures, 225°C and 300°C, while their conventional donor analogues required reaction temperatures of up to 475°C to obtain any appreciable reactivity. The nonaromatic hydroaromatics were essentially completely converted in 15 minutes at 380°C, e.g. ISO was 100% converted under hydrogen and 98.4% converted under nitrogen, and HHA was 90% converted under hydrogen and 98% converted under nitrogen. The high conversion obtained with the nonaromatic hydroaromatics is in comparison to the results

obtained at 380°C for the conventional hydrogen donor compound TET and OHA which did not convert under either nitrogen or hydrogen at 15 minutes, while DHA showed 2.1% conversion under hydrogen and 3.0% under nitrogen at 380°C in 15 minutes. The nonaromatic hydroaromatics not only required lower reaction temperatures than the conventional donors, but required shorter reaction times at a given temperature to be very reactive.

KINETIC ANALYSIS AND ARRHENIUS PLOTS FOR THE THERMAL REACTION OF THE COMPOUNDS UNDER NITROGEN AND HYDROGEN.

Also this quarter, the apparent rate constant k and linear regression correlation coefficients were determined for the reactions under nitrogen and hydrogen for each given model compound at a particular reaction temperature by using equation (1) and the data presented in

$$\ln \lambda = -kt + \ln(100) \qquad (1)$$

Tables II.D.1 through II.D.15. The results that were obtained are summarized in Table II.D.16. As can be seen, the fit of the data to the pseudo-first-order reaction kinetics was excellent for all of the compounds under both atmospheres. The straight line correlation coefficient was greater than 0.93 for all the reactions, and usually greater than 0.96. For all of the compounds studied, under both nitrogen and hydrogen, the rate constant increased with an increase in temperature. In other words, as the reaction temperature increased the reactivity of the model compounds for dehydrogenation also increased.

For the reactions at 380°C under nitrogen, the rate constant for ISO was 366 times greater than that of TET; for the reactions under hydrogen, the rate constant for ISO was 228 times greater than that of TET. For the reactions involving the three-ring series compounds at 380°C, under nitrogen the rate constant for HHA was 144 times greater than that for DHA, while under hydrogen it was 100 times greater. OHA was completely unreactive at 380°C under

both nitrogen and hydrogen at reaction times up to 90 minutes, so that no rate constant could be determined. At 380°C under nitrogen, the apparent rate constant for ISO was slightly more than that which was obtained for HHA, 0.27 versus 0.24; while in a hydrogen atmosphere the rate constant for ISO was nearly 2.5 times greater than that of HHA, 0.34 versus 0.14.

Arrhenius plots were developed for the five model compounds under both nitrogen and hydrogen by using the apparent rate constant data in Table II.D.16, and equation (2). From the

$$\ln k = \ln k_o - E_a/RT \qquad (2)$$

linear regression of this data, values for the activation energy, E_a, and frequency factor, k_o, were determined. These values are summarized in the last column of Table II.D.16. The fit of all the data to the Arrhenius plots was excellent, as evidenced by the straight line correlation coefficients all being 0.95 or greater.

For the reactions of the model compounds under nitrogen, the activation energy and frequency factors showed the following trend: OHA $\cong$ TET > DHA > ISO > HHA. For the reactions of the model compounds under hydrogen the activation energy and frequency factors showed the following trend: OHA > TET > ISO > HHA > DHA.

DETERMINATION OF GIBBS FREE ENERGY FOR THE THERMAL REACTIONS

Plots of the Gibbs free energy versus temperature were also obtained this quarter by using the values of the Arrhenius parameters, and the thermodynamic formulation of the activated complex theory, e.g. equation (3).

$$\Delta G = E_a - RT(1+\beta) - RT \ln(k_o/T) \qquad (3)$$

Figure II.D.1 is a plot of the Gibbs free energy (ΔG) of reaction over a temperature range of 127°C to 577°C for the reactions of the five model compounds in a nitrogen atmosphere. One of the most striking features of this plot is that the two nonaromatic

atmosphere. One of the most striking features of this plot is that the two nonaromatic hydroaromatics, ISO and HHA, have much lower values for ΔG than their conventional hydrogen donor analogues over the temperature range, except at very high temperatures (T > 475°C) where the values for all the compounds are similar. This plot, and associated theory, is a useful tool to explain the observed experimental orders of reactivity of the model hydrogen donor compounds. For a given temperature, those reactions having the lowest (most negative) values for ΔG will proceed in the most spontaneous fashion. For example, at a reaction temperature of 380°C under nitrogen, ISO and HHA were very reactive when compared to TET, DHA, and OHA. As is shown in Figure II.D.1, ISO and HHA have much lower values for ΔG than those for their conventional hydrogen donor analogues. The experimental reactivity ranking for the conventional donors at 380°C is DHA > TET > OHA, which is also what is predicted in Figure II.D.1. Figure II.D.1 also shows that OHA should always be the least reactive compound, which indeed was what was observed experimentally.

Figure II.D.2 is a plot of the Gibbs free energy versus temperature for the reaction of the five model compounds in a hydrogen atmosphere. Again, the nonaromtic hydroaromatics, ISO and HHA, have much lower values for ΔG than their conventional hydrogen donor analogues, and therefore, are predicted to be more reactive compounds. This conclusion was supported by the experimental results obtained in a hydrogen atmosphere. At 380°C, based upon the values of the Gibbs free energy in hydrogen, the reactivity of the conventional donors should be TET > DHA > OHA, which was also the order of reactivity observed experimentally.

Another important feature of Figure II.D.2 is the relatively flat slope of DHA. This suggests that at higher temperatures in a hydrogen atmosphere, DHA should be much less

reactive than either OHA or TET. The prediction that DHA should be less reactive at higher temperatures was supported experimentally. In examining the reactions in hydrogen at 60 minutes at 450°C, TET was converted ~80% , OHA was converted ~57% , while DHA was converted less than 30% .

The agreement between the experimentally observed thermal reactivity and behavior of the five model compounds studied, under both nitrogen and hydrogen, and the Gibbs free energy plots, as well as the first-order kinetic modeling, shows that the activated complex theory is useful for modeling the experimental reaction system.

Table II.D.1. Thermal Reaction Products from Isotetralin at 225°C

Reaction Conditions	Weight Percent Recovered				
	NAP	1,2-DHN	1,4-DHN	TET	ISO
ISO, 225°C					
HYDROGEN:					
2 MIN	0.0	0.0	1.7(0.3)	0.0	98.3(0.3)
30 MIN	0.0	0.0	2.4(0.1)	0.0	97.6(0.1)
60 MIN	0.0	0.0	3.5(0.2)	0.0	96.5(0.2)
90 MIN	0.0	0.0	4.3(0.1)	0.0	95.7(0.1)
NITROGEN:					
2 MIN	0.0	0.0	2.8(0.3)	0.0	97.2(0.3)
30 MIN	0.0	0.0	3.9(0.1)	0.0	96.1(0.1)
60 MIN	0.0	0.0	4.1(0.8)	0.0	95.9(0.8)
90 MIN	0.0	0.0	6.4(3.8)	0.0	93.6(3.8)
120 MIN	0.0	0.0	7.8(1.4)	0.0	92.2(1.4)

Table II.D.2. Thermal Reaction Products from Isotetralin at 300°C

Reaction Conditions	Weight Percent Recovered				
	NAP	1,2-DHN	1,4-DHN	TET	ISO
ISO, 300°C					
HYDROGEN:					
2 MIN	0.7(0.04)	0.7(0.05)	11.9(0.2)	0.0	86.7(0.2)
15 MIN	0.0	trace	15.6(0.5)	0.0	84.4(0.5)
30 MIN	0.0	1.0(0.1)	15.6(0.5)	0.0	83.4(0.5)
60 MIN	0.0	6.1(2.1)	25.8(3.7)	5.7(2.1)	62.4(9.0)
90 MIN	0.0	10.6(0.7)	27.9(0.5)	8.8(1.0)	52.7(2.2)
NITROGEN:					
2 MIN	0.6(0.04)	0.6(0.04)	11.0(0.3)	0.0	87.8(0.3)
15 MIN	0.0	0.0	12.4(3.7)	0.0	87.6(3.7)
30 MIN	0.0	0.0	15.4(0.8)	0.0	84.6(0.8)
60 MIN	0.0	0.0	23.1(0.8)	0.0	76.9(0.8)
90 MIN	0.0	0.0	30.9(0.5)	0.0	69.1(0.5)

Table II.D.3. Thermal Reaction Products from Isotetralin at 380°C

Reaction Conditions	Weight Percent Recovered				
	NAP	1,2-DHN	1,4-DHN	TET	ISO
ISO, 380°C					
HYDROGEN:					
2 MIN	2.2(0.2)	3.1(0.7)	39.1(1.8)	3.3(1.5)	52.4(2.9)
5 MIN	7.3(1.0)	9.4(4.2)	56.8(4.8)	8.5(3.2)	18.0(3.6)
10 MIN	30.4(0.4)	15.2(1.1)	35.2(0.4)	15.9(1.8)	3.3(0.6)
15 MIN	30.5(0.5)	23.8(4.6)	27.9(12.3)	17.8(6.0)	0.0
30 MIN	52.6(2.3)	10.0(2.6)	26.8(3.7)	10.6(1.2)	0.0
60 MIN	61.1(2.1)	11.5(1.7)	1.1(0.3)	26.3(3.5)	0.0
NITROGEN:					
2 MIN	3.6(0.1)	0.0	48.4(0.3)	1.6(0.1)	46.4(0.3)
5 MIN	5.6(0.4)	0.9(0.3)	67.7(0.9)	0.3(0.2)	25.5(0.9)
10 MIN	17.4(0.5)	2.3(0.3)	73.2(2.0)	1.2(0.4)	5.9(2.0)
15 MIN	23.4(0.4)	2.5(0.6)	70.3(0.7)	2.2(0.3)	1.6(0.2)
30 MIN	55.1(1.5)	4.6(0.5)	36.7(1.0)	3.6(0.4)	0.0
60 MIN	78.2(0.6)	4.8(0.2)	13.8(0.6)	3.2(0.3)	0.0

Table II.D.4. Thermal Reaction Products from Tetralin at 380°C

Reaction Conditions	Weight Percent Recovered				
	NAP	1,2-DHN	1,4-DHN	t-DEC	TET
TET, 380°C					
HYDROGEN:					
15 MIN	0.0	0.0	0.0	0.0	100.0
30 MIN	0.7(0.1)	1.0(0.1)	2.1(0.3)	0.0	96.2(2.3)
60 MIN	trace	0.0	trace	5.3(0.9)	94.7(0.9)
90 MIN	0.0	0.0	7.3(0.2)	6.3(0.1)	86.4(0.4
NITROGEN:					
15 MIN	0.0	0.0	0.0	0.0	100.0
30 MIN	0.8(0.2)	0.0	0.0	0.0	99.2(3.8)
60 MIN	0.6(0.1)	1.6(0.3)	2.0(0.6)	0.0	96.8(0.9)
90 MIN	1.0(0.03)	2.3(0.2)	3.1(0.4)	0.0	93.6(0.5)

Table II.D.5. Thermal Reaction Products from Tetralin at 425°C

Reaction Conditions	Weight Percent			
	NAP	1,2-DHN	1,4-DHN	TET
TET, 425°C				
HYDROGEN:				
2 MIN	0.0	4.8(0.3)	6.2(0.4)	89.0(0.6)
15 MIN	0.0	3.5(0.2)	8.6(0.1)	87.9(0.3)
30 MIN	0.9(0.1)	12.3(0.1)	32.0(1.0)	54.8(1.0)
60 MIN	1.9(0.2)	6.1(0.2)	61.7(5.4)	30.3(5.2)
NITROGEN:				
2 MIN	1.3(0.4)	4.6(0.4)	7.9(1.6)	86.2(1.7)
15 MIN	1.2(0.02)	12.5(0.6)	6.3(0.6)	80.0(1.2)
30 MIN	1.9(0.1)	8.6(0.3)	33.9(1.5)	55.6(1.7)
60 MIN	1.8(0.1)	8.5(1.2)	52.1(3.0)	37.6(2.0)

Table II.D.6. Thermal Reaction Products from Tetralin at 450°C

Reaction Conditions	Weight Percent			
	NAP	1,2-DHN	1,4-DHN	TET
TET, 450°C				
HYDROGEN:				
2 MIN	0.0	10.9(0.6)	11.8(1.5)	77.3(1.7)
15 MIN	1.2(0.1)	12.0(0.1)	53.9(0.5)	32.9(0.4)
30 MIN	2.2(0.3)	8.4(0.8)	63.9(0.3)	25.5(0.7)
60 MIN	5.0(0.5)	5.4(0.4)	68.0(1.4)	21.6(1.3)
90 MIN	8.3(0.3)	8.7(0.1)	74.8(1.0)	8.2(0.5)
NITROGEN:				
2 MIN	trace	10.4(0.6)	5.0(0.3)	84.6(0.3)
15 MIN	2.0(1.3)	23.8(1.5)	18.6(3.7)	55.6(4.4)
30 MIN	10.0(3.4)	22.4(5.4)	35.7(3.9)	31.9(1.7)
60 MIN	55.4(3.4)	5.7(0.6)	28.5(1.9)	10.4(1.2)

Table II.D.7. Thermal Reaction Products from Octahydroanthracene at 425°C

Reaction Conditions	Weight Percent			
	ANT	DHA	THA	OHA
OHA, 425°C				
HYDROGEN:				
2 MIN	0.0	0.0	0.0	100.0
15 MIN	0.0	0.0	trace	100.0
30 MIN	trace	1.6(0.2)	2.5(0.4)	96.0(0.6)
60 MIN	7.1(1.0)	5.4(0.3)	trace	87.5(1.3)
NITROGEN:				
2 MIN	0.0	0.0	0.0	100.0
15 MIN	0.0	0.0	trace	100.0
30 MIN	1.4(0.1)	2.4(0.7)	2.1(0.4)	94.1(1.1)
60 MIN	2.0(0.4)	7.4(0.5)	5.1(1.0)	85.4(1.0)

Table II.D.8. Thermal Reaction Products from Octahydroanthracene at 450°C

Reaction Conditions	Weight Percent			
	ANT	DHA	THA	OHA
OHA, 450°C				
HYDROGEN:				
2 MIN	0.0	0.0	0.0	100.0
15 MIN	1.9(0.4)	1.5(0.4)	4.6(1.3)	91.1(1.8)
30 MIN	5.8(3.6)	12.2(3.2)	20.5(1.4)	61.5(5.8)
60 MIN	7.9(0.1)	17.4(0.1)	31.3(0.6)	43.4(0.8)
NITROGEN:				
2 MIN	0.0	0.0	0.0	100.0
15 MIN	0.0	4.2(0.6)	0.0	95.8(0.6)
30 MIN	3.3(0.6)	14.7(1.2)	11.9(1.4)	70.1(2.7)
60 MIN	6.4(1.3)	12.4(2.3)	22.0(3.6)	59.2(2.6)

Table II.D.9. Thermal Reaction Products from Octahydroanthracene at 475°C

Reaction Conditions	Weight Percent			
	ANT	DHA	THA	OHA
OHA, 425°C				
HYDROGEN:				
2 MIN	0.0	0.0	0.0	100.0
15 MIN	1.7(0.4)	4.7(1.6)	12.8(3.6)	80.8(1.7)
30 MIN	5.2(1.2)	31.9(6.1)	23.0(7.8)	39.9(3.0)
60 MIN	18.3(0.9)	27.4(2.2)	39.9(1.1)	14.4(2.4)
NITROGEN:				
2 MIN	0.0	0.0	0.0	100.0
15 MIN	0.6(0.3)	8.0(0.3)	8.8(1.8)	82.6(0.9)
30 MIN	5.1(0.5)	32.8(1.0)	25.5(1.6)	36.6(2.2)
60 MIN	16.5(0.5)	36.4(1.2)	34.4(1.8)	12.7(3.0)

Table II.D.10. Thermal Reaction Products from Dihydroanthracene at 380°C

Reaction Conditions	Weight Percent		
	ANT	THA	DHA
DHA, 380°C			
HYDROGEN:			
2 MIN	1.4(1.6)	0.0	98.6(1.6)
15 MIN	2.1(0.1)	0.0	97.9(0.1)
30 MIN	5.7(0.5)	2.2(0.8)	92.1(2.1)
60 MIN	3.6(0.2)	4.2(0.2)	92.2(0.4)
90 MIN	5.1(0.1)	7.6(0.1)	87.3(0.2)
NITROGEN:			
2 MIN	0.4(0.3)	0.0	99.6(0.3)
15 MIN	3.0(0.3)	0.0	97.0(0.3)
30 MIN	5.0(0.6)	0.0	95.0(0.6)
60 MIN	9.6(0.9)	0.0	90.4(0.9)

Table II.D.11. Thermal Reaction Products from Dihydroanthracene at 425°C

Reaction Conditions	Weight Percent		
	ANT	THA	DHA
DHA, 425°C			
HYDROGEN:			
2 MIN	2.9(0.6)	0.0	97.1(0.6)
15 MIN	7.5(0.3)	0.0	92.5(0.3)
30 MIN	8.8(1.1)	0.0	91.2(1.1)
60 MIN	11.1(1.2)	3.2(1.4)	85.7(0.4)
NITROGEN:			
2 MIN	11.6(0.3)	0.0	88.4(0.3)
15 MIN	30.1(1.5)	0.0	69.9(1.5)
30 MIN	35.8(0.9)	0.0	64.2(0.9)
60 MIN	60.3(5.3)	0.0	39.7(5.3)

Table II.D.12. Thermal Reaction Products from Dihydroanthracene at 450°C

Reaction Conditions	Weight Percent		
	ANT	THA	DHA
DHA, 450°C			
HYDROGEN:			
2 MIN	4.4(0.3)	2.0(2.3)	93.6(2.4)
15 MIN	12.5(0.3)	2.5(0.5)	85.0(0.7)
30 MIN	12.7(0.1)	4.8(0.2)	82.5(0.3)
60 MIN	20.5(1.0)	8.3(0.5)	71.3(1.2)
NITROGEN:			
2 MIN	26.9(9.2)	0.0	73.1(9.2)
15 MIN	47.8(3.8)	0.0	52.2(3.8)
30 MIN	75.1(0.5)	0.0	24.9(0.5)
60 MIN	91.5(0.5)	1.9(0.4)	6.6(0.5)

Table II.D.13. Thermal Reaction Products from Hexahydroanthracene at 225°C

Reaction Conditions	Weight Percent			
	ANT	DHA	THA	HHA
HHA, 225°C				
HYDROGEN:				
2 MIN	0.0	1.2(0.4)	0.5(0.2)	98.3(0.2)
30 MIN	0.0	2.1(0.1)	1.2(0.2)	96.6(0.2)
60 MIN	0.0	2.1(0.5)	1.4(0.2)	96.5(0.6)
90 MIN	0.0	2.7(0.2)	1.6(0.1)	95.7(0.3)
120 MIN	0.0	3.2(0.3)	2.6(0.1)	94.2(0.3)
NITROGEN:				
2 MIN	0.0	1.9(0.4)	0.8(0.1)	97.3(0.3)
30 MIN	0.0	3.1(0.01)	2.1(0.1)	94.8(0.1)
60 MIN	0.0	5.8(0.6)	3.9(0.5)	90.3(1.1)
90 MIN	0.0	7.5(2.4)	5.2(1.2)	87.2(3.5)

Table II.D.14. Thermal Reaction Products from Hexahydroanthracene at 300°C

Reaction Conditions	Weight Percent			
	ANT	DHA	THA	HHA
HHA, 300°C				
HYDROGEN:				
2 MIN	0.0	4.5(0.3)	2.4(0.2)	93.1(0.4)
15 MIN	0.0	6.1(0.2)	2.3(0.2)	91.6(0.4)
30 MIN	0.0	14.4(0.3)	4.2(0.1)	81.4(0.2)
60 MIN	0.0	20.6(0.2)	13.0(0.3)	66.4(0.5)
NITROGEN:				
2 MIN	0.0	0.0	5.5(0.2)	94.5(0.2)
15 MIN	0.0	6.7(0.1)	2.2(0.1)	91.1(0.1)
30 MIN	0.0	16.0(3.1)	6.7(2.6)	77.3(5.7)
60 MIN	0.0	31.4(1.7)	9.9(1.3)	58.7(1.1)

Table II.D.15. Thermal Reaction Products from Hexahydroanthracene at 380°C

Reaction Conditions	Weight Percent				
	ANT	DHA	THA	OHA	HHA
HHA, 380°C					
HYDROGEN:					
2 MIN	0.0	29.3(0.5)	9.8(0.4)	0.0	60.9(0.7)
5 MIN	6.2(0.1)	51.2(0.5)	6.2(0.2)	0.0	36.4(0.2)
10 MIN	8.3(1.3)	60.8(5.9)	16.5(8.9)	0.0	14.4(1.7)
15 MIN	2.1(0.2)	78.0(8.1)	9.8(5.1)	0.0	10.0(5.3)
30 MIN	7.0(0.8)	83.1(4.4)	8.6(1.8)	0.0	1.3(0.4)
60 MIN	5.2(0.9)	68.5(3.9)	20.2(3.7)	4.5(1.3)	1.7(0.4)
NITROGEN:					
2 MIN	0.0	40.8(3.3)	12.2(1.0)	0.0	47.0(4.3)
5 MIN	0.0	76.0(3.6)	6.3(2.0)	0.0	17.7(1.5)
10 MIN	1.3(1.5)	83.4(1.8)	4.5(2.9)	0.0	10.8(2.6)
15 MIN	3.5(0.1)	85.1(0.2)	9.3(0.1)	0.0	2.0(0.1)
30 MIN	15.0(2.7)		13.5(2.9)	0.0	trace
60 MIN	11.2(0.6)	71.5(10.0)	3.1(0.03)	0.0	0.0
		85.7(0.6)			

Table II.D.16. Apparent Rate Constants and Arrhenius Parameters for the Model Compound Reactivity Studies

Reaction Conditions	Apparent Rate Constant (k)	Correlation Coefficent for Rate Constant	Arrhenius Parameters
DHA			
NITROGEN:			
380°C	0.00167	0.99861	Ea/R=21,975
425°C	0.01426	0.98632	k_o=6.85x10^{11}
450°C	0.04372	0.99624	r=0.99995
HYDROGEN:			
380°C	0.00140	0.95254	Ea/R=8,147
425°C	0.00233	0.96478	k_o=3.41x10^{2}
450°C	0.00505	0.96901	r=0.95251
HHA			
NITROGEN:			
225°C	0.00142	0.98638	Ea/R=10,623
300°C	0.00864	0.99179	k_o=1.92x10^{6}
380°C	0.24067	0.98263	r=0.97395
HYDROGEN:			
225°C	0.00040	0.93072	Ea/R=12,238
430°C	0.00641	0.98657	k_o=1.64x10^{7}
380°C	0.14086	0.99267	r=0.99592
OHA			
NITROGEN:			
425°C	0.00271	0.97051	Ea/R=27,006
450°C	0.00944	0.96606	k_o=1.67x10^{14}
475°C	0.03606	0.98928	r=0.99918
HYDROGEN:			
425°C	0.00226	0.96235	Ea/R=28,224
450°C	0.01468	0.98485	k_o=9.59x10^{14}
475°C	0.03335	0.99130	r=0.97972
ISO			
NITROGEN:			
225°C	0.00055	0.93852	Ea/R=12,780
300°C	0.00337	0.94919	k_o=4.76x10^{7}
380°C	0.27118	0.99846	r=0.95691
HYDROGEN:			
225°C	0.00041	0.93232	Ea/R=13,990
430°C	0.00652	0.97460	k_o=4.90x10^{8}
380°C	0.34391	0.99992	r=0.98695
TET			
NITROGEN:			
380°C	0.00074	0.96811	Ea/R=27,027
425°C	0.01578	0.98755	k_o=7.69x10^{14}
450°C	0.03698	0.99932	r=0.99233
HYDROGEN:			
380°C	0.00151	0.94641	Ea/R=19,712
425°C	0.01975	0.98308	k_o=2.27x10^{10}
450°C	0.02405	0.94310	r=0.96353

Ea = Activation Energy
R = Universal gas constant
k_o = frequency factor
r = correlation coefficient

Figure II.D.1.

PLOT OF GIBBS FREE ENERGY vs TEMPERATURE.
NITROGEN ATMOSPHERE

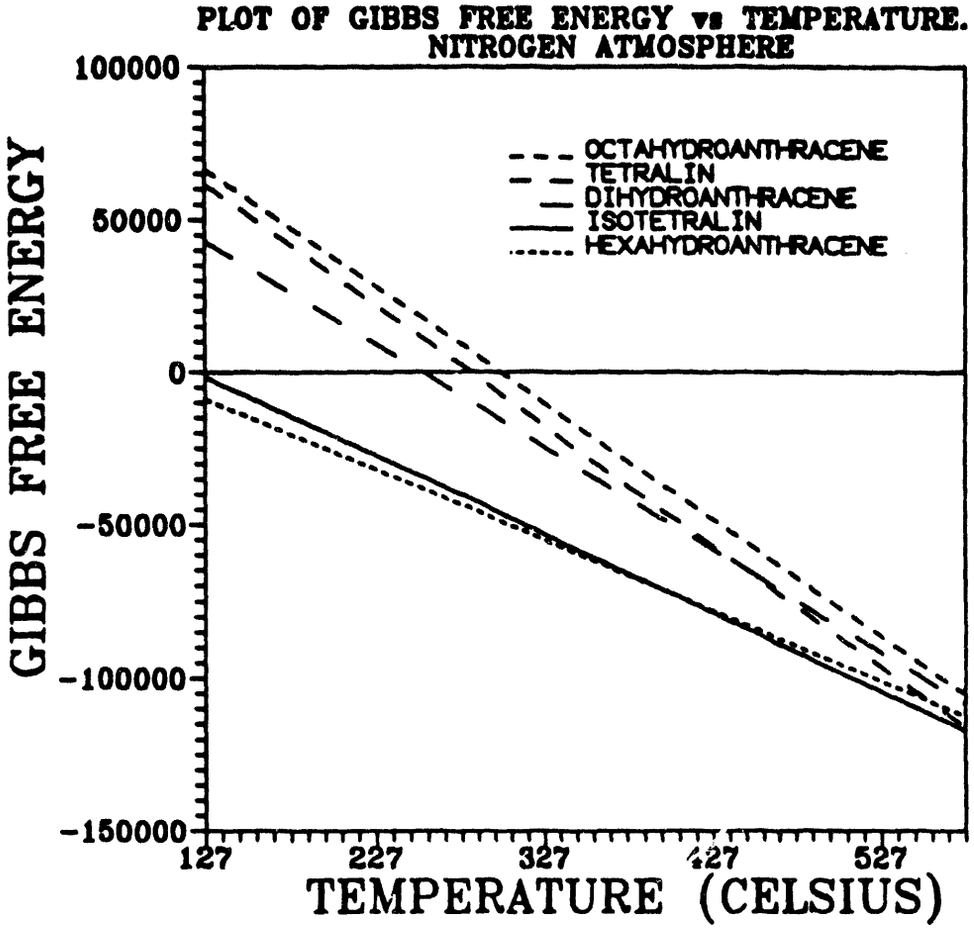

Figure II.D.2.

PLOT OF GIBBS FREE ENERGY vs TEMPERATURE.
HYDROGEN ATMOSPHERE

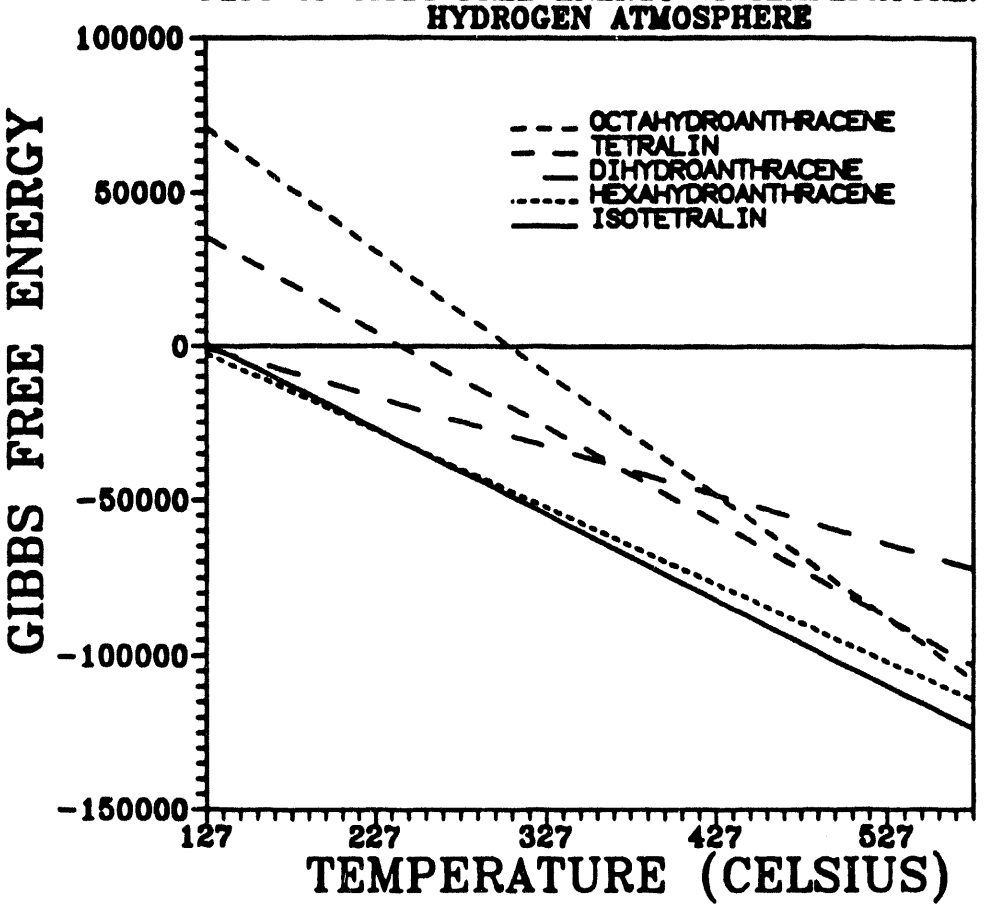

DATE
FILMED

4/6/94

END